Journal of Power Sources 195 (2010) 6287–6293

Contents lists available at ScienceDirect

Journal of Power Sources

journal homepage: www.elsevier.com/locate/jpowsour

Effect of black catalyst ionomer content on the performance of passive DMFC

Mohammad Ali Abdelkareem [a], Takuya Tsujiguchi [b], Nobuyoshi Nakagawa [b,*]

[a] Advanced Technology Centre (ATEC), Gunma University, 1-5-1 Tenjin, Kiryu, Gunma 375-8515, Japan
[b] Department of Chemical and Environmental Engineering, Gunma University, 1-5-1 Tenjin, Kiryu, Gunma 375-8515, Japan

ARTICLE INFO

Article history:
Received 4 January 2010
Received in revised form 16 April 2010
Accepted 21 April 2010
Available online 28 April 2010

Keywords:
Passive DMFC
Black catalyst
Nafion ionomer content
ECSA
Catalyst utilization

ABSTRACT

The effect of the ionomer content in the catalyst layers of both the anode and the cathode with the black catalyst on the performance of a passive DMFC was investigated in order to increase the power output of the passive DMFC. *In situ* cyclic voltammetry has been carried out to evaluate the electrochemically active surface area, ECSA and the catalyst utilization. Under the passive conditions, ionomer content had a significant effect on both the mass transport and the ECSA. The optimum ionomer content was affected by the operating current density whether at anode or at cathode. Under low current density region, i.e., activation over voltage region, 20 wt.% showed the highest performance at the anode and the cathode, and the cell performance in this region was varied in accordance with the results of the ECSA. Under high current density region, i.e., mass transport over voltage region, lower ionomer content, 10 and 15 wt.%, had the highest cell performance at the anode and the cathode, respectively. The decrease in the optimum ionomer content at high current density was related to the low mass transport of methanol at the anode, and the flooding at the cathode at the high ionomer contents. The optimum ionomer content whether at anode or at cathode was 20 wt.%, from the power density point of view. The catalyst utilization was 10% and 25% at optimum conditions at the cathode and the anode respectively.

1. Introduction

There is a great interest in the development of direct methanol fuel cells (DMFCs), because of their high theoretical energy density that is suitable for mobile electric devices and automobiles. However, the commercialization of the DMFC was hindered by many obstacles such as the methanol crossover, MCO and the high over voltage at the electrodes [1–5]. The microstructure of the catalyst layer plays a key factor in fuel cell performance. The reaction and the mass transport as well as ohmic over-voltages of the DMFC are affected by the ionomer content in the catalyst layer where the ionomer prepares the active reaction sites, the so-called three-phase boundary, by contacting it with the catalyst particles. In this three-phase boundary layer, the ionomer layer acts as channels for ion transport between the membrane and the reaction sites, while the open pores act as channels for the mass transport of the reactants and/or products to or from the reaction sites, respectively. With increasing the ionomer content, the channels for proton transport increase but the open pores available for mass transport decrease.

The addition of the ionomer affects the number of reaction sites, where hydrogen protons are generated or consumed, and the channels for the ionic path based on the mixing and the distribution structures of the catalyst with the ionomer. These structures determine the effective ionic conductivity of the catalyst layer and the number of effective reaction sites.

At the same time, the addition of the ionomer affects the mass transport whether to or from the reaction active sites or to the electrolyte membrane. With the increasing ionomer content, the catalyst utilization will increase. A further increase in the ionomer content results in the formation of a thick ionomer layer on the catalyst, thereby the access of the reactants or the products to or from the active sites decreases, therefore, the catalyst utilization decreases. Hence, there is an optimum ionomer content which is a compromise among the high number of effective reaction sites, the high effective ionic conductivity and the low mass transport resistance [6–10]. Moreover, the ionomer content influences the hydrophobic and hydrophilic pore distribution in the catalyst layer so its content affects the transport of the liquid and gas phases [11].

In a PEMFC, many studies have been carried out to investigate the optimum ionomer content [6–15]. The best results have been reported at different ionomer loadings by different researchers, and it generally ranged from 30 to 40 wt.% of the catalyst loading.

The optimum ionomer content in the catalyst layer of DMFC is considered to be different from that in the PEMFC because of the high mass transport resistance. At the anode of DMFC, methanol has a low diffusion coefficient, compared to that of hydrogen gas in the PEMFC, as well as the difficulties of the releasing of the CO_2. At the cathode, MCO, in DMFC, not only causes a mixed potential and flooding, but also consumes the oxygen required for the oxy-

* Corresponding author. Tel.: +81 277 30 1458; fax: +81 277 30 1457.
E-mail address: nakagawa@cee.gunma-u.ac.jp (N. Nakagawa).

0378-7753/$ – see front matter © 2010 Elsevier B.V. All rights reserved.
doi:10.1016/j.jpowsour.2010.04.070

Table 1
List of the previous studies that investigated the optimum ionomer content in the catalyst layer for the DMFC.

Electrode	Catalyst	Preparation method	Catalyst loading ($mg\,cm^{-2}$)	Conc. (M)	Temp. (K)	Operation mode	Optimum NAF (wt.%)	Ref.
Anode	PtRu black (1:1)	C paper treated	–	2 M	383	Active	36	Chu et al. [16]
		Decal	2+/−0.3	1 M	353	Active	6.5	Thomas et al. [17]
		Decal	3.9	1 M	353	Active	7	Dohle et al. [18]
		–	3	2 M	353	Active	4	Kim et al. [19]
		Decal/CCM	3	1 M	348	Active	15	Zhao et al. [26]
	PtRu (53%)/C	–	3	2 M	353	Active	60	Kim et al. [19]
	PtRu (40%)/C	CCM	1	1	353	Active	25	Krishnamurthy et al. [20]
	Pt40 Ru20/CNT	C cloth, vacuum filtration	4	1 M	–	Active	63	Jeng et al. [25]
	PtRu (60%)/C	Decal	2	1 M	343	Active	20–40	Wannek et al. [27]
	Pt20 Ru10/C	Spraying, C paper treated	2	1 M	313	Active	>60	Birry et al. [28]
Cathode	Pt black	Decal	2.5+/−0.5	1 M	353	Active	10.5	Thomas et al. [17]
		CCM, C paper and MPL	–	–	–	Active	33	Krishnamurthy et al. [21]
	Pt/C	CCM, C cloth and MPL	1.2	H2	333	Active	22	Liu et al. [22]
	Pt (20 & 40%)/C	CCM, C paper and MPL	2	1 M	353	Active	33	Krishnamurthy et al. [20,21]

CCM, catalyst coated membrane; MPL, micro porous layer.

gen reduction reaction. Both results in additional oxygen transport limitations at the cathode surface.

Many studies have been done to determine the optimum ionomer content for the DMFCs [16–27] as shown in Table 1. As obvious from the table, the optimum ionomer content varied from one study to another depending on the preparation method, catalyst type, diffusion media and also the operating conditions. The catalyst layers with the same composition produced on different substrates, i.e., (decal sheets, gas diffusion layers or directly on membranes), resulted in different mass transport limitations. Therefore, different optimum ionomer content was expected. The black catalyst prepared by the decal methods realized a low optimum ionomer content of less than 15 wt.% [17,18,26]. This is because, in the decal method, catalyst ink with the ionomer was first applied on a non-porous sheet without any permeation loss of the ionomer. Higher ionomer contents were required in the other preparation methods [16,21] and/or for the supported catalyst [19–21,25,26,28], in which a catalyst ink was applied on a porous diffusion media, i.e., a microporous layer (MPL), carbon paper or carbon cloth. A large portion of the ionomer permeates through these layers, therefore, a relatively large amount of the ionomer was used in the catalyst layer. If a vacuum was used during the preparation, the ionomer loss by permeation would be increased and higher ionomer content was required [25]. The supported catalyst is nanoparticles finely distributed on a carbon support that requires a higher ionomer content to provide enough contact between the catalyst and the ionomer [21]. Moreover, the operating conditions, such as cell temperature [11,22] reactant flow rate [22] and methanol concentration affect the mass transport, therefore, the optimum ionomer content.

Recently, a passive DMFC that absorbs methanol from a built in methanol reservoir by an osmotic action and breathes O_2 from the surrounding air by natural diffusion and convection, has been demonstrated and investigated by some researchers [29–42]. Under the low cell temperatures around 298 K used for passive conditions, the resistance to mass transport becomes high in comparison to that at high temperature around 353 K, used for the active conditions. At the cathode, the accumulation of water blocks the openings of the cathode and blocks the O_2 supply, and at a high current density, flooding is quite severe and significantly depresses the cell performance. At the anode, the low diffusion of methanol and the CO_2 release, at low cell temperature, limit the methanol supply. Under these high mass transport resistances, the optimum ionomer content for the passive DMFC is expected to be lower than that for the active conditions. Up to now, there has been no report about the optimum ionomer content in the passive DMFC.

Under the passive conditions, carbon cloth was widely used as the diffusion layer to enhance the mass transport and black catalyst was used to increase the catalyst activity. *In situ* cyclic voltammetry measurements were usually done at the actual operating temperature. This study has been carried out to clarify the optimum ionomer content in a passive DMFC using the black catalyst, PtRu at the anode, Pt at the cathode and carbon cloth as the diffusion layer. Polarization and *in situ* cyclic voltammetry measurements have been carried out to investigate the effect of the ionomer content on the cell performance and evaluate the electrochemically active surface area ECSA, respectively.

2. Experimental

2.1. MEA preparation

The MEA, which uses carbon cloth (35% Teflonized, ElectroChem, Inc.) as the anode and cathode backing layers, was prepared in the following manner: 3–4 $mg\,cm^{-2}$ of carbon black, Ketjen black, containing 10% PTFE, a microporous layer MPL, was prepared on the surface of the carbon cloth.

Pt black of 2 nm particle size (HiSPEC 1000, Johnson Matthey Fuel Cells, Co., Ltd.) and PtRu black of 2.72 nm particle size (HiSPEC 6000, Johnson Matthey Fuel Cells, Co., Ltd.) were used as the catalyst for the cathode and the anode, respectively. Catalyst ink was prepared by dispersing an appropriate amount of the catalyst in a solution of de-ionized water, isopropyl alcohol and a 5 wt.% Nafion solution (Wako, Inc.). The ink was then precipitated on the surface of the carbon cloth with the MPL using a micropipette to form the catalyst layer. The catalyst loading was around 4 $mg\,cm^{-2}$ in each electrode. For the anode catalyst layer, five different electrodes containing 10, 15, 20, 30 and 40 wt.% of the ionomer were prepared as the anodes while the ionomer content in the cathode catalyst layer was fixed at 30 wt.%. For the cathode catalyst layer, four different electrodes containing 10, 15, 20 and 30 wt.% of the ionomer were prepared as the cathodes in which the ionomer content in the anode catalyst layer was fixed at 20 wt.%.

Nafion 112 was used as the electrolyte membrane. The MEA was then fabricated by sandwiching the membrane between the anode and the cathode and hot pressing them at 408 K and 5 MPa for 3 min.

2.2. Electrochemical measurements

2.2.1. Measurement of cell performance

The MEA was placed in a plastic holder as shown in Fig. 1. In the anode compartment, a methanol reservoir, 22 mm wide, 22 mm

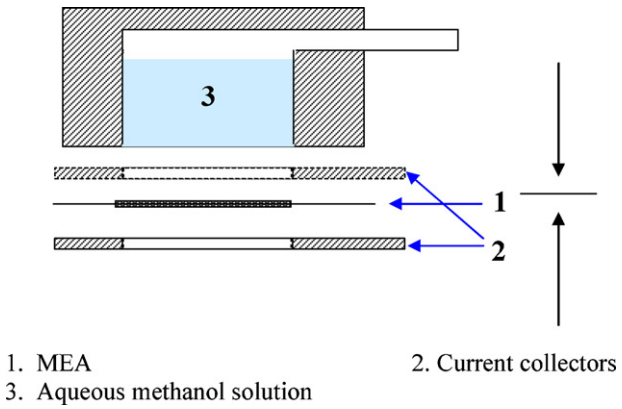

Fig. 1. Schematic diagram of a passive DMFC.

long and 25 mm deep was prepared. The MEA was sandwiched between two current collectors, which were stainless steel plates of 2 mm thickness with open channels for the passage of the fuel and oxidant. The open area ratio for the active electrode was 73%.

In this study, all the experiments were conducted in the completely passive mode with the surrounding air at the ambient conditions of 297 K and 1 atm. A methanol solution with different concentration 1–4 M, was fed into the reservoir by a syringe through the open tube. The current–voltage *i*–*V*, characteristics were measured from OCV to zero voltage at the scan rate of 1 mV s^{-1}. These measurements were conducted using an electrochemical measurement system (HAG-5010, Hokuto Denko, Co., Ltd.).

2.2.2. In situ cyclic voltammetry and impedance

During the electrode and MEA fabrication processes, it is not guaranteed that all of the catalyst particles will be available for electrochemical reaction due to either insufficient contact with the polymer electrolyte or electrical isolation of the catalyst particles [43]. *In situ* cyclic voltammograms are useful in assessing the ECSA used under actual operating conditions. Therefore, the measurements have been carried out under room temperature 298 K, to mimic the actual operating conditions of the passive DMFC.

The MEA was placed in a cell holder with flow channels in both the anode and cathode (FC-005-01SP, Electro Chem Co., Ltd.). The electrochemical active surface areas ECSA, of the anode and the cathode catalysts were determined by CO stripping and hydrogen adsorption–desorption measurements, respectively. For the CO stripping, the fuel cell cathode used as both the reference electrode, dynamic hydrogen electrode (DHE) and counter electrode, while the fuel cell anode was the working electrode. The cathode was purged with nitrogen for 10 min at 1 l min^{-1} then switched to humidified hydrogen at 0.1 l min^{-1} and ambient pressure. Two Molar methanol was flowed to the anode at 4.8 ml min^{-1}, maintaining the cell voltage at 0.1 V for 1 h. Methanol at the anode was then purged with nitrogen, 1 l min^{-1} for 20 min, and then switched to de-aerated water at 4.8 ml min^{-1} for 40 min. The cell voltage was maintained in the all stages at 0.1 V. The potential was scanned at 20 mV s^{-1} between 0.1 and 1.2 V. The integrated peak area of the CO electro-oxidation was used to calculate the ECSA of the anode. For the hydrogen adsorption–desorption analysis, the fuel cell anode was used as both reference electrode, a dynamic hydrogen electrode and counter electrode, while the fuel cell cathode was the working electrode. The anode was purged with nitrogen for 10 min then switched to humidified hydrogen at 0.1 l min^{-1} and ambient pressure, while de-aerated water was flowed on the cathode side at 4.8 ml min^{-1}. The potential was scanned at 20 mV s^{-1} between 0.05 and 1.2 V. The average integrated peaks area of the hydrogen adsorption–desorption curves was used to calculate the ECSA of the cathode.

ECSA was calculated based on the following equation:

$$\mathrm{ECSA} = \frac{Q_1}{Q_2.G}$$

where Q_1 is the charge amount calculated from the integration of the CV curves for the CO desorption electro-oxidation or the average hydrogen adsorption–desorption in coulombs (C), Q_2 is the charge amount required to oxidize a monolayer of CO on the alloy catalyst of 4.20 C m^{-2} or a single layer of saturated coverage of hydrogen on the Pt surface area of 2.1 C m^{-2} and G represents the total metal loading (g) in the electrode [43].

The catalyst utilization was calculated by dividing the ECSA by the specific surface area of the catalysts, SSA. The specific surface area SSA, of the electro catalysts can be calculated from the mean particle size by the following equation, assuming all the catalyst particles have a spherical shape [44]:

$$\mathrm{SSA} = \frac{6}{\rho d}$$

where d is the mean particle size and ρ is the catalyst density.

Electrochemical impedance spectra (EIS) were measured for the MEAs containing different anode ionomer contents using an electrochemical measurement system (HAG-5010, Hokuto Denko Co. Ltd.). One molar methanol solution (1 ml min^{-1}) was supplied to the fuel cell anode at 298 K while a continuous stream of hydrogen was fed to the fuel cell cathode to form a DHE and to facilitate the removal of the permeated water. Impedance spectra for the working electrode was measured based on the DHE in the complete fuel cell under potentiosatatic mode (0.4 V) over the frequency range 1 kHz–10 mHz.

3. Results and discussion

3.1. Effect of the ionomer content in the anode catalyst layer

3.1.1. Effect of the ionomer content in the anode catalyst layer on the ECSA and the impedance

The *in situ* cyclic voltammograms have been carried out to clarify the effect of the ionomer content on the electrochemically active surface area ECSA. Fig. 2 shows the CO stripping of the anode electrodes with different ionomer contents i. e., 10, 20, 30 and 40 wt.%. As noted from the figure, the CO stripping area increased with the increasing ionomer content up to 20 wt.% and then it decreased with a further increase in the ionomer content. At the same time, the onset potential for the CO adsorption oxidation decreased with the increasing ionomer content to 20 wt.%, then increased with a further increase in the ionomer content. It was 244 mV at 10 wt.%, 234 mV at 15 wt.% (not shown in the figure), 231 mV at 20 wt.% and 248 mV at both the 30 and 40 wt.%. Based on the CO stripping area, both the ECSA and the catalyst utilization were calculated and plotted versus the ionomer content as shown in Fig. 3. As clarified from the figures, the electrode with 20 wt.% ionomer had the highest ECSA, highest catalyst utilization and the lowest onset potential for the CO adsorption oxidation. With the increasing ionomer content from 10 to 20 wt.%, the contact between the catalyst and ionomer increased, therefore, the apparent proton conductivity of the catalyst layer increased, and more catalyst contributed to the electrochemical reaction thus the ECSA increased, the catalyst activity increased and the onset potential of the CO adsorption oxidation decreased. Although the dispersion of the catalyst increased, i.e., the contact of the catalyst particles with the ionomer content increased, with the increasing ionomer content to 30 and 40 wt.%, ECSA decreased. The decrease in the ECSA would be related to the isolation of some of the catalyst particles by a thick

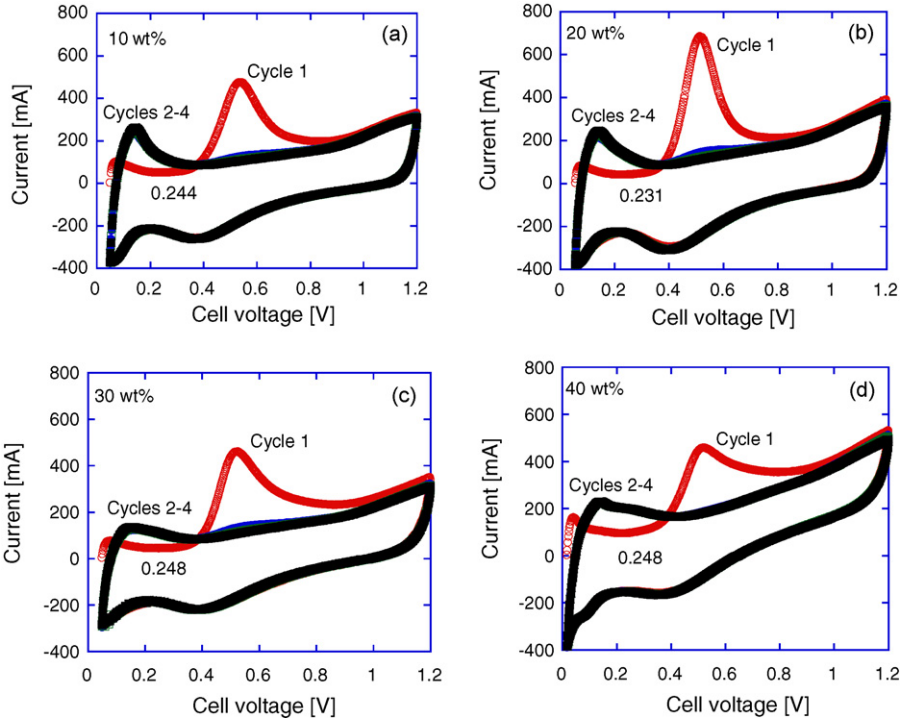

Fig. 2. CO stripping of the anode electrodes with the different ionomer contents of (a) 10 wt.%, (b) 20 wt.%, (c) 30 wt.% and (d) 40 wt.%.

layer of the ionomer around them at 30 and 40 wt.% ionomer. This thick ionomer layer acted as a barrier for the mass transport of the reactants and products to or from the catalyst particles, therefore, ECSA decreased. The effect of the mass transport resistance on ECSA appeared at low ionomer content 20 wt.%, compared to that under active condition, usually 30 wt.% as shown in Table 1, which would be related to performing the measurement at low cell temperature 298 K, compared with that used under active conditions 353 K.

The impedance measurements have been carried out for the different anode ionomer contents as shown in Fig. 4. As noted from the figure, the lowest resistance to the electro-oxidation of methanol occurred at 20 wt.% ionomer content as clear from the size of the arcs at the different ionomer contents. These results were in accordance with that of the ECSA.

3.1.2. *Effect of the ionomer content in the anode catalyst layer on the i–V performance*

Fig. 5 shows the current voltage curves for the MEAs containing the different ionomer contents in the anode catalyst layer of 10, 20, 30 and 40 wt.% at 3 M. As noted from the figure, except 20 wt.% ionomer content, which showed the highest cell performance at the entire cell potential, the effect of the other ionomer contents, 10, 30 and 40 wt.%, on cell performance was dependent on the current density. At low current density region, i.e., lower than 40 mA cm^{-2}, 30 wt.% showed the highest performance among them followed by 40 and 10 wt.% while, at high current density region i.e., higher than 100 mA cm^{-2}, 10 wt.% showed highest performance followed by 30 and 40 wt.%, and even it was better than that obtained at 20 wt.% at zero.

At low current density, cell operated under activation over voltage region, therefore, the variation of the performance was related to the variation of the ECSA.

At high current density, cell operated under mass transport over voltage region. The number of the open pores, used as channels for mass transport, formed at low ionomer content would be higher

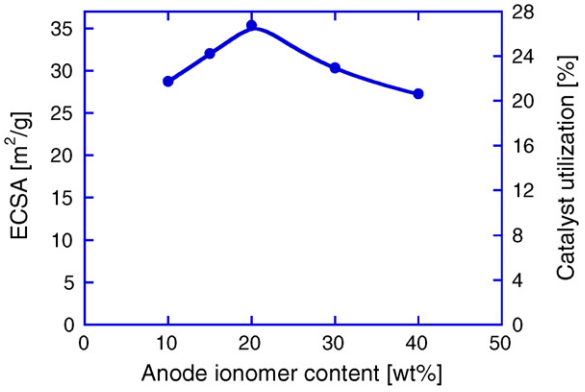

Fig. 3. The effect of the ionomer content on the ECSA and the catalyst utilization of the different anodes.

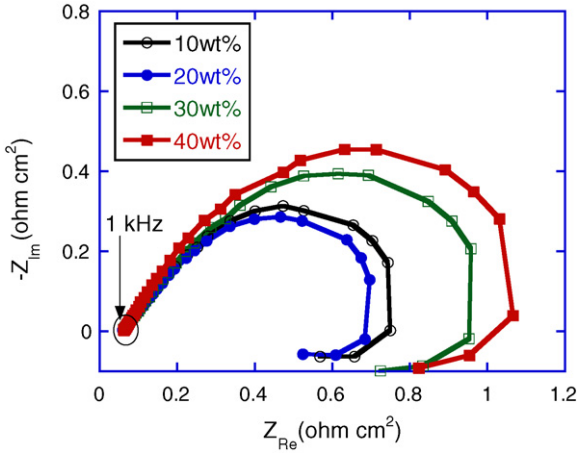

Fig. 4. Effect of Nafion content in the anode catalyst layers on impedance response in the Nyquist form at 0.4 versus DHE, with 1 M methanol, flow rate: 1 ml min^{-1} at 298 K.

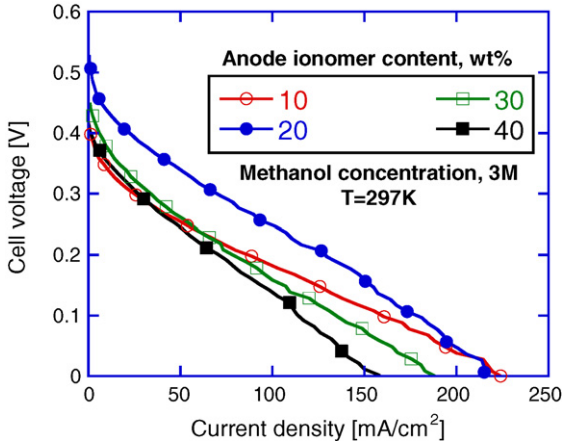

Fig. 5. The current voltage curves for the MEAs containing different ionomer contents in the anode catalyst layer of 10, 20, 30 and 40 wt.% at 3 M.

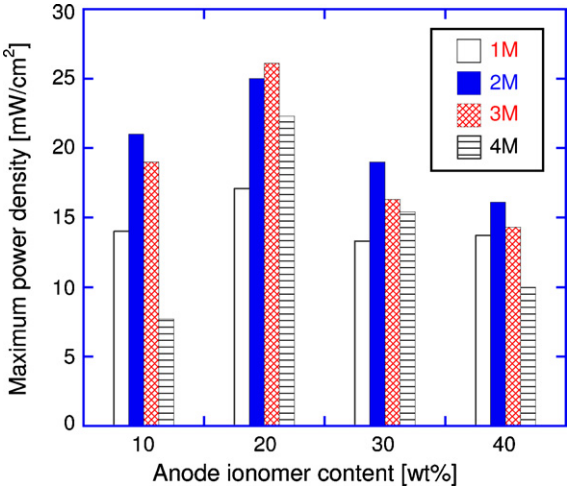

Fig. 6. The effect of the ionomer content in the anode catalyst layer on the maximum power density at different methanol concentrations.

than that formed at high ionomer content. Therefore, 10 wt.% had the lowest mass transport over voltage, and thus the highest performance. The significant effect of the ionomer content on the cell performance at the high current density would be related to the high resistance to the mass transport under the passive operating conditions.

The performance of the different MEAs, prepared with the different ionomer contents in the anode catalyst layer, has been measured under passive conditions using different methanol concentrations from 1 to 4 M. Fig. 6 shows the maximum power density of each methanol concentration versus the ionomer content. It was clear from the figure that the power density at the different methanol concentrations increased with increasing ionomer content until 25 mW cm^{-2} at 20 wt.% and then decreased with the further increase in the ionomer content. The optimum methanol concentration at the different ionomer contents was 2 and 3 M. The highest maximum power density at 20 wt.% would be related to the high catalyst activity at 20 wt.% as clear from the ECSA and the impedance measurements.

3.2. Effect of the ionomer content in the cathode catalyst layer

3.2.1. Effect of the ionomer content in the cathode catalyst layer on ECSA

Fig. 7 shows the *in situ* cyclic voltammetry curves of the hydrogen adsorption–desorption of the cathode catalyst elec-

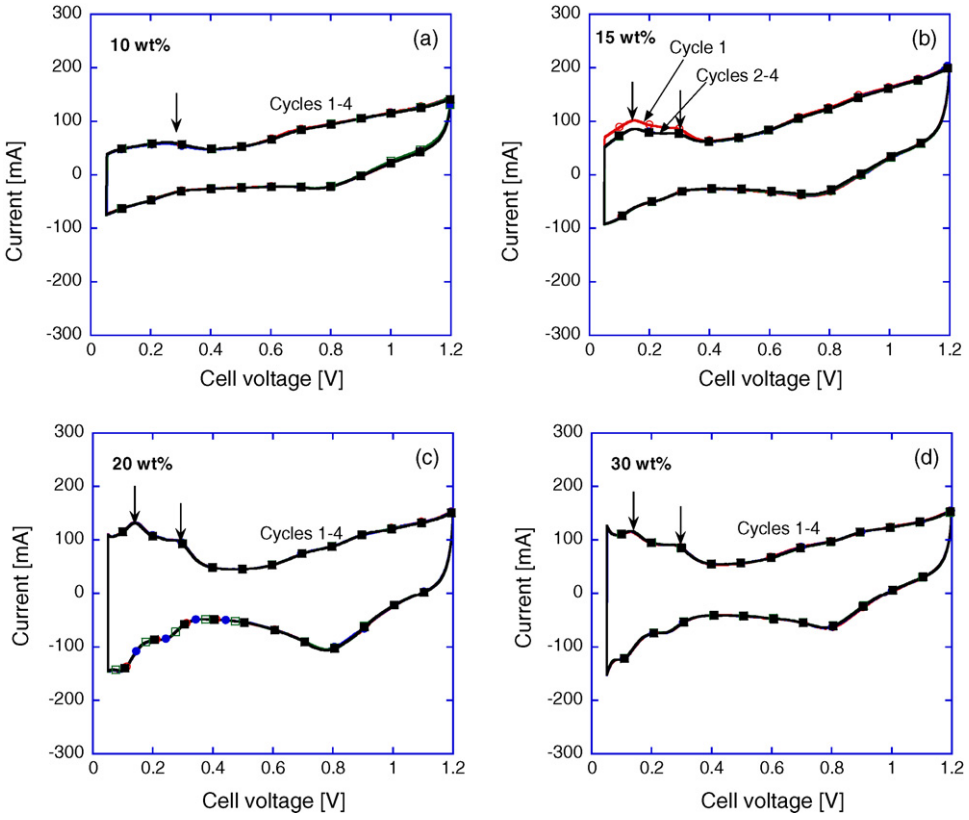

Fig. 7. Hydrogen adsorption–desorption of the cathode catalyst electrodes prepared with the different ionomer contents of (a) 10 wt.%, (b) 15 wt.%, (c) 20 wt.% and (d) 30 wt.%.

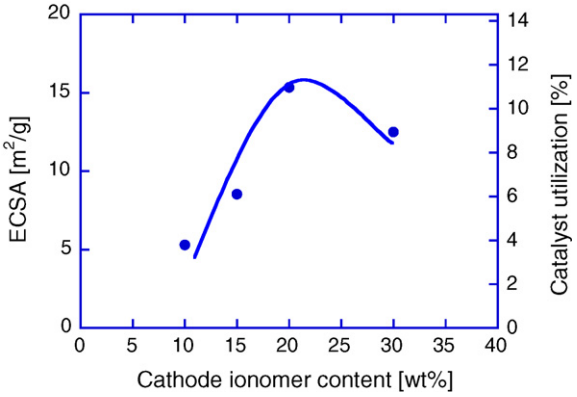

Fig. 8. The effect of the ionomer content on the ECSA and the catalyst utilization of the different cathodes.

trodes prepared with the different ionomer contents of 10, 15, 20 and 30 wt.%. As noted from the figure, the number of adsorption–desorption peaks, indicated by the arrows in the figure, increased from one peak appeared at 10 wt.%, to two peaks at the higher ionomer contents. Both the ECSA and the catalyst utilization were calculated based on the average of the adsorption–desorption areas in Fig. 7 and plotted versus the ionomer content as shown in Fig. 8. The ECSA and the catalyst utilization increased with the increasing ionomer content from 10 to 20 wt.% then decreased with the further increase in the ionomer content to 30 wt.%.

As already described for the anode, at the low ionomer content of 10 wt.%, the apparent ionic conductivity of the catalyst layer was low, therefore, a small portion of the catalyst participated in the electrochemical reaction. With increasing the ionomer content, the catalyst distribution improved and the contact between the catalyst and the ionomer increased, therefore, more catalyst with different crystal facets participated in the electrochemical reaction.

The catalyst utilization at the low ionomer contents of 10 and 15 wt.% was quite low, but it significantly increased when the ionomer content increased to 20 wt.%. This situation did not appear in the case of the PtRu catalyst at the anode and we do not know the reason for the difference between these two cases until now.

3.2.2. Effect of ionomer content in the cathode catalyst layer on i–V performance

Fig. 9 shows the current voltage curves for the MEAs containing different ionomer contents in the cathode catalyst layer of 10, 15, 20 and 30 wt.% at 3 M. At a low current density region, i.e., lower

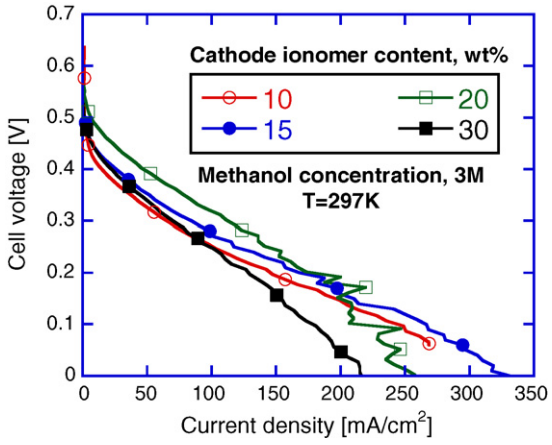

Fig. 9. The current voltage curves for the MEAs containing different ionomer contents in the cathode catalyst layer of 10, 15, 20 and 30 wt.% at 3 M.

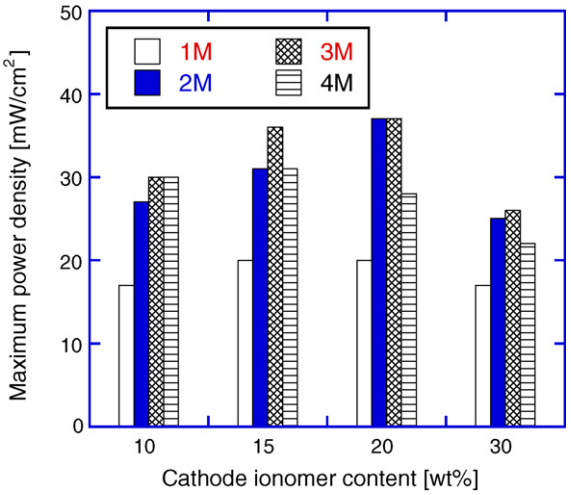

Fig. 10. The effect of the ionomer content in the cathode catalyst layer on the maximum power density at different methanol concentrations.

than 40 mA cm^{-2}, the highest performance was obtained at 20 wt.%, while at high current density region, i.e., higher than 100 mA cm^{-2}, the highest performance was obtained at 15 wt.%. As clear from the figure, cell performance was affected by the ionomer content in the cathode catalyst layer and this effect was dependent on the current density.

As already described in the case of the anode side, at low current density, cell operated under activation over voltage region, therefore, catalyst activity, i.e., ECSA, governed the cell performance. At high current density, cell operated under mass transport over voltage region, therefore, lower ionomer content, i.e., 15 wt.% showed the highest cell performance. The fluctuations in the current density at 20 wt.% would be related to the flooding at high current density. The increasing in the ionomer content enhanced the flooding at high current density; therefore, cell performance depressed and 15 wt.% showed better performance than that obtained at 20 wt.%.

The performance of the different MEAs, prepared with different ionomer contents in the cathode catalyst layer, has been measured under the passive condition using different methanol concentrations from 1 to 4 M. Fig. 10 shows the maximum power density for each methanol concentration versus the ionomer content. It was clear from the figure that, the power density increased from 30 to 38 mW cm^{-2} with the increasing ionomer content from 10 to 20 wt.%, then it decreased with a further increase in the ionomer content. The optimum methanol concentration for all the MEAs was 3 M.

The degree of the change in the performance with the changing ionomer content, which was low in comparison to that of the ECSA, shown in Fig. 10, would be related to the flooding which depressed the cell performance.

It was clear that the optimum ionomer content was affected by the current density region whether at the anode or at the cathode, which makes the passive DMFC more complicated than the active one. Although improvement of the cell performance by optimizing the ionomer content in both the anode and cathode occurred, the catalyst utilization was low at around 10% at the cathode and 25% at the anode.

4. Conclusions

The effect of the ionomer content on the performance of a passive DMFC using a black catalyst at anode and cathode has been investigated. Polarization and *in situ* cyclic voltammetry measurements have been carried out to investigate the effect of the ionomer

content on the cell performance and catalyst utilization, respectively. The following conclusions were drawn.

1) Under passive conditions, from the maximum power density point of view, the optimum ionomer content was 20 wt.%, whether at anode or at cathode, which was considered to be lower than that used under active conditions. This was related to the high resistance to mass transport under passive conditions.
2) The optimum ionomer content was affected by the operating conditions, i.e., current density, whether at anode or at cathode. Under low current density, i.e., activation over voltage region, cell performance governed by the catalyst activity, i.e., ECSA. Under high current density, i.e., mass transport over voltage region, catalyst layer with low ionomer content showed the highest cell performance.
3) The catalyst utilization was 10% and 25 wt.% at optimum conditions at the cathode and the anode respectively, this low value this would be related to the moderate passive operating conditions.

References

[1] J.D. Morse, Int. J. Energy Res. 31 (2007) 576–602.
[2] A.S. Arico, S. Srinivasan, V. Antonucci, Fuel Cells 1 (2001) 133–161.
[3] T. Schultz, K. Su Zhou, Sundmacher, Chem. Eng. Technol. 24 (2001) 1223–1233.
[4] J.G. Liu, T.S. Zhao, R. Chen, C.W. Wong, Electrochem. Commun. 7 (2005) 288.
[5] J.G. Liu, T.S. Zhao, Z.X. Liang, R. Chen, J. Power Sources 153 (2006) 61–67.
[6] G. Sasikumar, J.W. Ihm, H. Ryu, Electrochim. Acta 50 (2004) 601–605.
[7] R. Dillon, S. Srinivasan, A.S. Aricò, V. Antonucci, J. Power Sources 127 (2004) 112.
[8] C.K. Dyer, J. Power Sources 106 (2002) 31.
[9] S. Gottesfeld, Fuel Cells 5 (2005) 45.
[10] X. Ren, M.S. Wilson, S. Gottesfeld, J. Electrochem. Soc. 143 (1996) L12.
[11] A.D. Blasi, V. Baglio, T. Denaro, V. Antonucci, A.S. Aricò, J. New Mater. Electrochem. Syst. 11 (2008) 165.
[12] C. Lamy, S. Rousseau, E.M. Belgsir, C. Coutanceau, J.-M. Leger, Electrochim. Acta 49 (2004) 3901.
[13] S.J. Lee, S. Mukerjee, J. McBreen, Y.W. Rho, Y.T. Kho, T.H. Lee, Electrochim. Acta 43 (1998) 3693.
[14] E. Antolini, L. Giorgi, A. Pozio, E. Passalacqua, J. Power Sources 77 (1999) 136.
[15] E. Passalacqua, F. Lufrano, G. Squadrito, A. Patti, L. Giorgi, Electrochim. Acta 46 (2001) 799.
[16] Y. Chu, Y. Shul, W. Cho, S. Woo, H. Han, J. Power Sources 118 (2003) 334.
[17] S.C. Thomas, X. Ren, S. Gottesfeld, J. Electrochem. Soc. 146 (1999) 4354.
[18] H. Dohle, H. Schmitz, T. Bewer, J. Mergel, D. Stolten, J. Power Sources 106 (2002) 313.
[19] J. Kim, H. Ha, I. Oh, S. Hong, H.N. Kim, H. Lee, Electrochim. Acta 50 (2004) 801.
[20] B. Krishnamurthy, S. Deepalochani, K.S. Dhathathreyan, Fuel Cells 8 (2008) 404–409.
[21] B. Krishnamurthy, S. Deepalochani, Int. J. Electrochem. Sci. 4 (2009) 386.
[22] F. Liu, C. Wang, Electrochim. Acta 52 (2006) 1417.
[23] R. Chen, T.S. Zhao, J.G. Liu, J. Power Sources 157 (2006) 351.
[24] T.S. Zhao, R. Chen, W.W. Yang, C. Xu, J. Power Sources 191 (2009) 185–202.
[25] K. Jeng, C. Chien, N. Hsu, W. Huang, S. Chiou, S. Lin, J. Power Sources 164 (2007) 33–41.
[26] X. Zhao, X. Fan, S. Wang, S. Yang, B. Yi, Q. Xin, G. Sun, Int. J. Hydrogen Energy 30 (2005) 1003–1010.
[27] C. Wannek, S. Neher, M. Vahlenkamp, J. Mergel, D. Stolten, J. Appl. Electrochem. 40 (2010) 29–38.
[28] L. Birry, C. Bock, X. Xue, R. McMillan, B. MacDougall, J. Appl. Electrochem. 39 (2009) 347–360.
[29] N. Nakagawa, K. Kamata, A. Nakazawa, M.A. Abdelkareem, K. Sekimoto, Electrochemistry 74 (3) (2006) 221–225.
[30] N. Nakagawa, M.A. Abdelkareem, K. Sekimoto, J. Power Sources 160 (2006) 105–115.
[31] M.A. Abdelkareem, N. Nakagawa, J. Power Sources 162 (2006) 114–123.
[32] M.A. Abdelkareem, N. Nakagawa, J. Power Sources 165 (2007) 685–691.
[33] M.A. Abdelkareem, N. Morohashi, N. Nakagawa, J. Power Sources 172 (2007) 659–665.
[34] N. Nakagawa, M.A. Abdelkareem, J. Chem. Eng. Jpn. 40 (2007) 1199–1204.
[35] Z. Guo, A. Faghri, J. Power Sources 160 (2006) 1142–1155.
[36] H.K. Kim, J. Power Sources 162 (2006) 1232–1235.
[37] Z. Guo, Y. Cao, J. Power Sources 132 (2004) 86–91.
[38] J. Liu, G. Sun, F. Zhao, G. Wang, G. Zhao, L. Chen, B. Yi, Q. Xin, J. Power Sources 133 (2004) 175–180.
[39] C.H. Lee, C.H. Park, S.Y. Lee, B.O. Jung, Y.M. Lee, Desalination 233 (2008) 210–217.
[40] J.J. Martin, W. Qian, H. Wang, V. Neburchilov, J. Zhang, D.P. Wilkinson, Z. Chang, J. Power Sources 164 (2007) 287–292.
[41] B. Bae, B.K. Kho, T. Lim, I. Oh, S. Hong, H.Y. Ha, J. Power Sources 158 (2006) 1256–1261.
[42] R. Chen, T.S. Zhao, W.W. Yang, C. Xu, J. Power Sources 175 (2008) 276–287.
[43] J. Zhang, PEM Fuel Cell Electrocatalysts and Catalyst Layers, 2008 Springer-Verlag London Limited, 2008, chapter 11.
[44] W. Chen, G. sun, J. Guo, X. Zhao, S. Yan, J. Tian, S. Tang, Z. Zhou, Q. Xin, Electrochim. Acta 51 (2006) 2391.